

ECAP

가

† . * . ** . ***

Finite Element Analysis for Behavior of Aluminum Alloy Embedding a Particle under Equal Channel Angular Pressing

S. C. Lee, S. R. Ha, K. T. Kim, H. S. Chung

Key Words : Composites(), Equal Channel Angular Pressing(가), Finite Element Analysis(), Porous Materials(), Weibull Fracture Probability()

Abstract

Behavior of aluminum alloy embedding a particle was investigated at room temperature under ECAP. Finite element analysis by using ABAQUS shows that ECAP is a useful tool for eliminating residual porosity in the specimen, and much more effective under friction condition. The simulation, however, shows considerably low density distributions for matrix near a particle at which rich defects may occur during severe deformation. Finite element results of effective strains and deformed shapes for matrix with a particle were compared with theoretical calculations under simple shear stress. Also, based on the distribution of the maximum principal stress in the specimen, Weibull fracture probability was obtained for particle sizes and particle-coating layer materials. The probability was useful to predict the trend of more susceptible failure of a brittle coating layer than a particle without an interphase in metal matrix composites.

1.

가 (severe plastic deformation) 가 ECAP 가
ECAP(Equal Channel Angular Pressing) 가 가

. ECAP

. Li Langdon⁽¹¹⁾ Valiev⁽¹²⁾

, ECAP 가
가

†
E-mail: yanus@postech.ac.kr
Tel: (054) 279-2838 FAX: (054) 279-2871

* 가
** (가)

*** ECAP 가
Chang⁽¹³⁾ 가

(14) ECAP 가 가 , ECAP 가 가

3.

3.1

ABAQUS⁽¹⁷⁾

ECAP 가

ECAP

(Φ) 90°

ECAP

(Ψ) 0°

ECAP

가

Fig. 1 ECAP

가

10mm×10mm×75mm

2720

4211 4

(plane strain reduced integration element, CPE4R)

ECAP

(defect)

0.9

(18)

Gurson (15)

ECAP

가

(plane strain)

가

(Weibull fracture probability)

10mm×10mm

10 vol%

3.56mm

가

Fig.

1(b)

5 vol%

2.52mm

0.15mm

2.

ECAP

2.1 Gurson

Al6061

ECAP

가

Gurson (15)

CuAl₂

Gurson

Table 1

0.9

Al6061

(19,20)

Al6061 : $\sigma_m = 80 + 172.64(\bar{\epsilon}_m^p)^{0.3103}$ (2)

copper : $\sigma_m = 149 + 479.97(\bar{\epsilon}_m^p)^{0.2433}$ (3)

Table 1 Material properties of various materials⁽¹⁹⁻²²⁾.

$$\Phi(\sigma, \bar{\epsilon}_m^p, D) = \left(\frac{q}{\sigma_m}\right)^2 + 2q_1(1-D) \cosh\left(-\frac{3q_2 p}{2\sigma_m}\right) - 1 - \{q_1(1-D)\}^2 = 0 \quad (1)$$

$$p = \sqrt{\frac{3}{2} \sigma'_{ij} \sigma'_{ij}} \quad (= \sigma_{kk} / 3)$$

$$q = \sqrt{3} \sigma'_{ij} \sigma'_{ij} / 2 \quad q_1 = 1.25$$

q₂ = 1 Tvergaard⁽¹⁶⁾가

q₁ q₂ 1 Gurson

Materials	Elastic Modulus(GPa)	Poisson's Ratio
Al6061	69.7	0.33
Copper	110.3	0.3
CuAl ₂	138	0.3
SiC	414	0.17

3.2

3.2.1

Fig. 2 ECAP

Al6061

Fig. 1(a)

ECAP

$D_0=0.99, f=0.1$

$D_0=0.97, f=0.1$

Fig. 2

4

A

가

가

C

가

D

Fig. 3

65mm

가

(Fig. 3(c)),

가 가

(Fig. 3(a,b)).

0.97

0.99

ECAP

1

ECAP

Fig. 4

ECAP

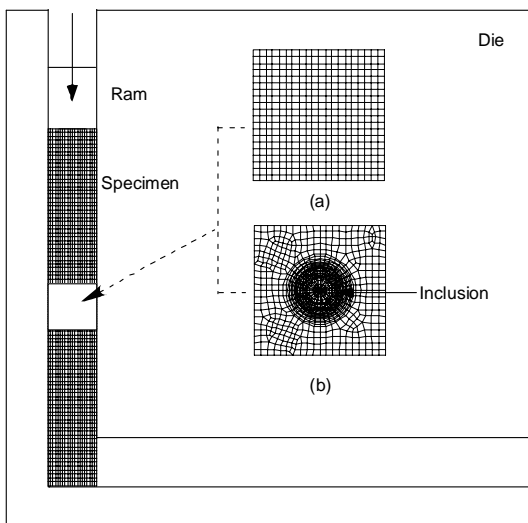


Fig. 1 A schematic drawing and finite element meshes for ECAP.

0.1

3.5

Fig. 5

가 0.99

가

ECAP

Fig. 1(b)

10 vol%

가

가

가

(defect)

Fig. 6 ECAP

가

Fig. 1 (a,b)

Iwahashi (6)

$$\varepsilon = \left[\frac{2 \cot\left(\frac{\Phi}{2} + \frac{\Psi}{2}\right) + \Psi \operatorname{cosec}\left(\frac{\Phi}{2} + \frac{\Psi}{2}\right)}{\sqrt{3}} \right] \quad (4)$$

(Φ) 90° ,

(Ψ) 0°

1.155

0.9399, $f=0.1$

1.223

$D_0=0.99$

$D_0=1$

$D_0=0.99, f=0.1$

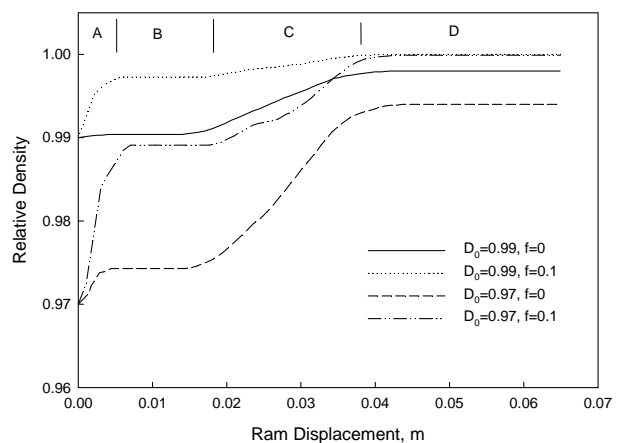


Fig. 2 Variation of relative density of specimen with ram displacement under ECAP.

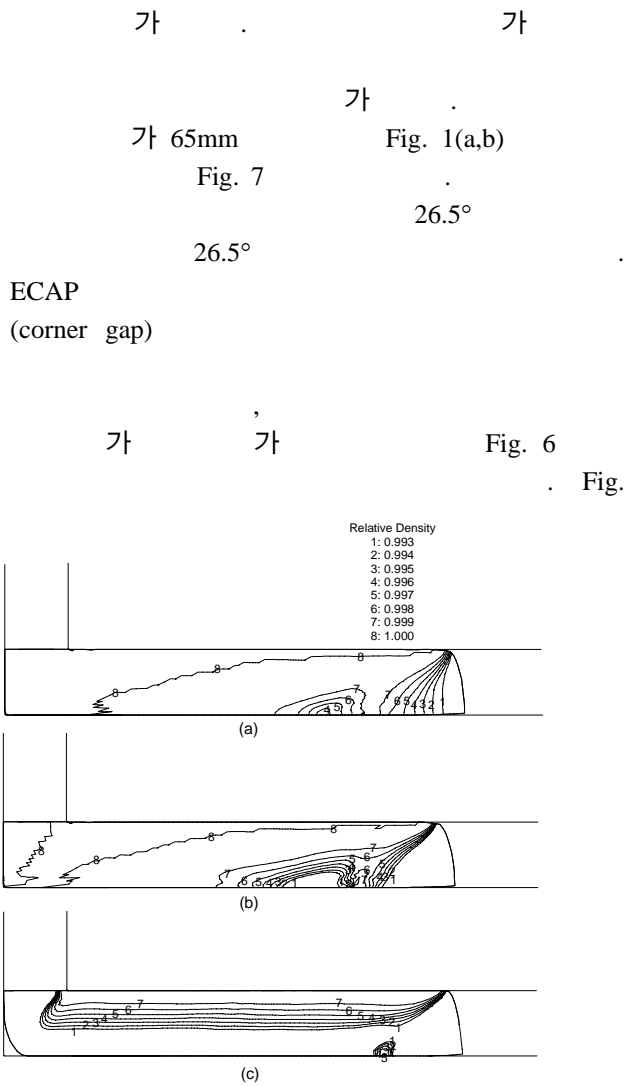


Fig. 3 Finite element calculations for distribution of relative density in the cases of (a) $D_0=0.99$, $f=0.1$, (b) $D_0=0.97$, $f=0.1$ and (c) $D_0=0.99$, $f=0$ under ECAP.

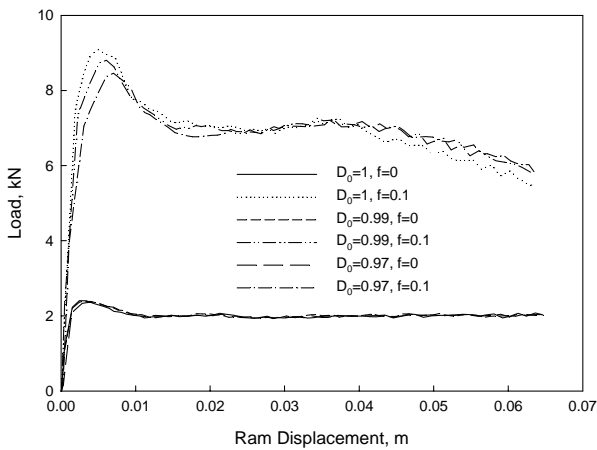


Fig. 4 Variation of pressing load with ram displacement for various initial densities and friction conditions.

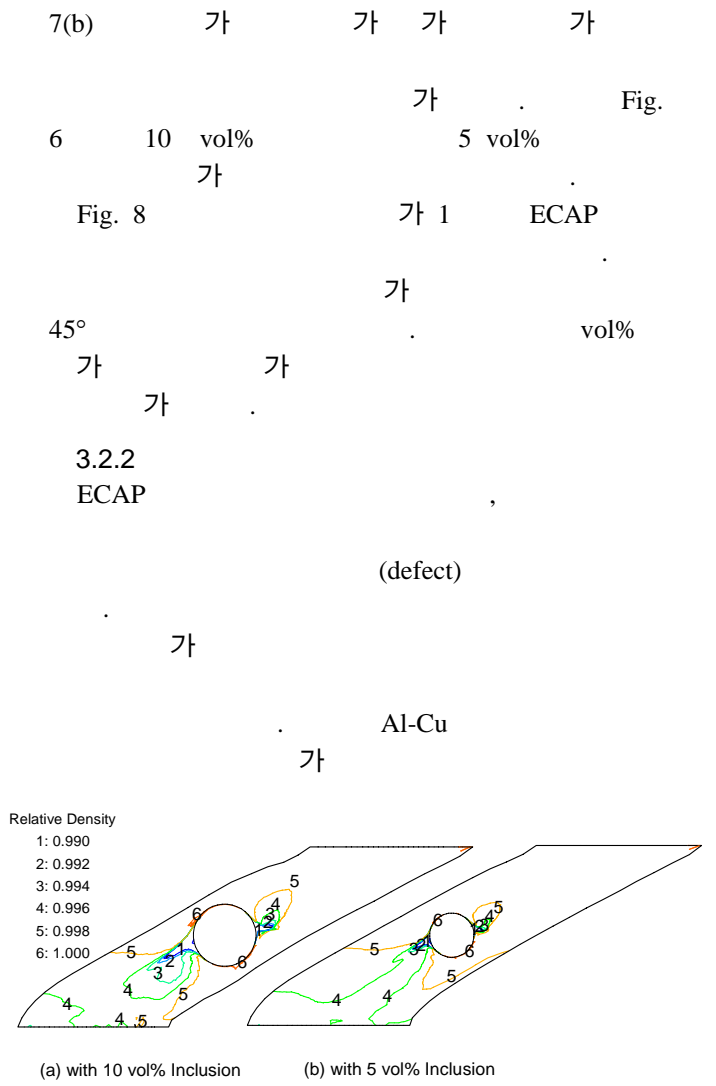


Fig. 5 Relative density contour plots of Al alloy with a SiC particle after ECAP.

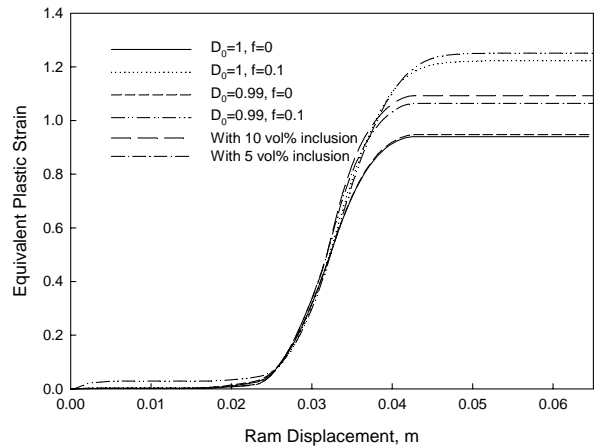


Fig. 6 Variation of effective plastic strain with ram displacement for unreinforced and a SiC particle-embedding Al alloy.

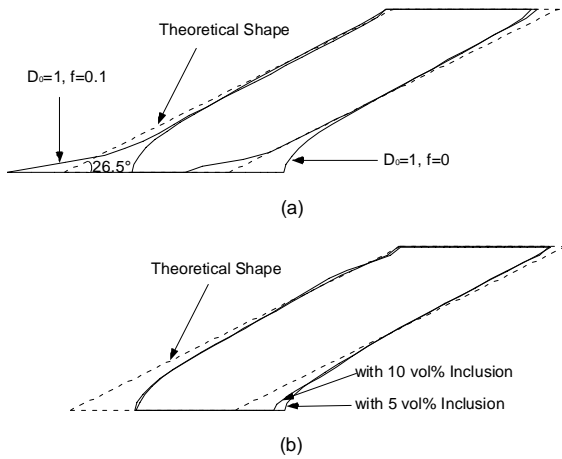


Fig. 7 Comparisons of final deformed shapes between finite element results and theoretical calculation for (a) unreinforced and (b) a SiC particle-embedding Al alloy.

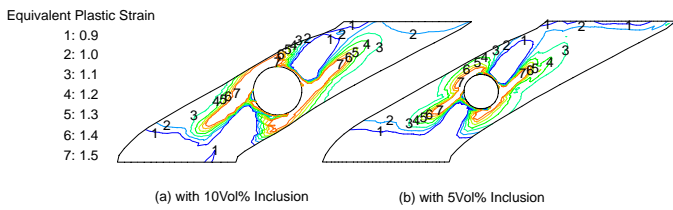


Fig. 8 Finite element calculations for distribution of effective plastic strain for Al alloy with a SiC particle after ECAP.

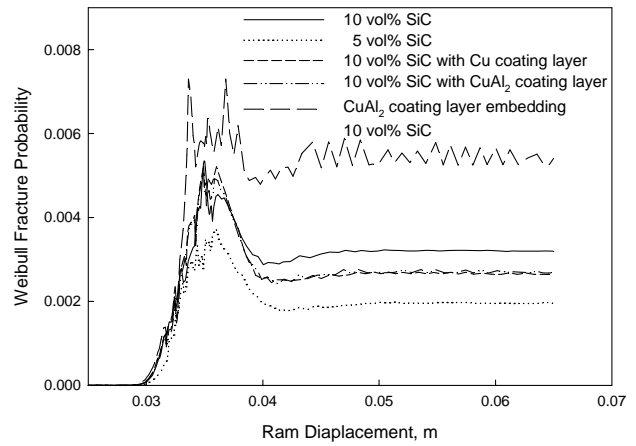


Fig. 9 Variation of Weibull fracture probability with ram displacement under ECAP.

$$m = \frac{1.2-1.8 \text{ GPa}}{3 \text{ to } 6} \quad (24)$$

ECAP

$$\sigma_0 = 1.2 \text{ GPa}, m = 3$$

가
(: 0.030~0.037m)

CuAl₂
CuAl₂
ECAP

CuAl₂
(defect)

(Weibull fracture probability)

V

4.

(maximum principal tensile stress) 가
(23)

Gurson

ECAP

$$P_f = 1 - \exp \left[- \frac{1}{V_0 (\sigma_0)^m} \int_{V: \sigma_1(r) > 0} (\sigma_1(r))^m dV \right] \quad (5)$$

가

$\sigma_1(r)$

(reference volume) V_0

ECAP

, V: $\sigma_1(r) > 0$

σ_0

가
ECAP
가
가
CuAl₂
ECAP
CuAl₂

(1) Shan, A., Moon, I. G., Ko, H. S. and Park, J. W., 1999, "Direct Observation of Shear Deformation During Equal Channel Angular Pressing of Pure Aluminum," *Scripta Mater.*, Vol. 41, No. 4, pp. 353~357.

(2) Saito, Y., Utsunomiya, H., Suzuki, H. and Sakai, T., 2000, "Improvement in the γ -value of Aluminum Strip by a Continuous Shear Deformation Process," *Scripta Mater.*, Vol. 42, pp. 1139~1144.

(3) Horita, Z., Fujinami, T. and Langdon, T. G., 2001, "The Potential for Scaling ECAP: Effect of Sample Size on Grain Refinement and Mechanical Properties," *Mater. Sci. Eng.*, Vol. A318, pp. 34~41.

(4) Furukawa, W., Horita, Z., Nemoto, M., Valiev, R. Z. and Langdon, T. G., 1996, "Microhardness Measurements and the Hall-Petch Relationship in an Al-Mg Alloy with Submicrometer Grain Size," *Acta Mater.*, Vol. 44, No. 11, pp. 4619~4629.

(5) Segal, V. M., 1995, "Materials Processing by Simple Shear," *Mater. Sci. Eng.*, Vol. A197, pp. 157~164.

(6) Iwahashi, Y., Wang, J., Horita, Z., Nemoto, M. and Langdon, T. G., 1996, "Principle of Equal-Channel Angular Pressing for the Processing of Ultra-fine Grained Materials," *Scripta Metall.*, Vol. 35, No. 2, pp. 143~146.

(7) Srinivasan, R., 2001, "Computer Simulation of the Equichannel Angular Extrusion (ECAE) Process," *Scripta Mater.*, Vol. 44, pp. 91~96.

(8) Prangnell, P. B., Harris, C. and Roberts, S. M., 1997, "Finite Element Modelling of Equal Channel Angular Extrusion," *Scripta Mater.*, Vol. 37, No. 7, pp. 983~989.

(9) Kim, H. S., Seo, M. H. and Hong, S. I., 2000, "On the Die Corner Gap Formation in Equal Channel

Angular Pressing," *Mater. Sci. Eng.*, Vol. A291, pp. 86~90.

(10) Seimiati, S. L., Delo, D. P. and Shell, E. B., 2000, "The Effect of Material Properties and Tooling Design on Deformation and Fracture during Equal Channel Angular Extrusion," *Acta Mater.*, Vol. 48, pp. 1841~1851.

(11) Li, Y. and Langdon, T. G., 2000, "Equal-channel Angular Pressing of an Al-6061 Metal Matrix Composite," *J. Mater. Sci.*, Vol. 35, pp. 1201~1204.

(12) Valiev, R. Z., Islamgaliev, R. K. and Kuzmina, N. F., Li, Y. and Langdon, T. G., 1999, "Strengthening and Grain Refinement in an Al-6061 Metal Matrix Composite through Intense Plastic Straining," *Scripta Mater.*, Vol. 40, No. 1, pp. 117~122.

(13) Chang, S. Y., Lee, K. S., Choi, S. H. and Shin, D. H., 2003, "Effect of ECAP on Microstructure and Mechanical Properties of a Commercial 6061 Al Alloy Produced by Powder Metallurgy," *J. Alloys Compd.*, Vol. 354, pp. 216~220.

(14) Chang, S. Y., Lee, K. S., Ryu, S. K., Park, K. T. and Shin, D. H., 2002, "Effect of Equal Channel Angular Pressing on the Distribution of Reinforcements in the Discontinuous Metal Matrix Composites," *Mater. Trans.*, Vol. 43, No. 4, pp. 757~761.

(15) Gurson, A. L., 1977, "Continuum Theory of Ductile Rupture by Void Nucleation and Growth-Part 1. Yield Criteria and Flow Rules for Porous Ductile Media," *J. Eng. Mat. Tech.*, Vol. 99, pp. 2~15.

(16) Tvergaard, V., 1982, "On Localization in Ductile Materials Containing Spherical Voids," *Int. J. Fracture*, Vol. 18, pp. 237~252.

(17) *ABAQUS User's I and II Manual*, Hibbit, Karlsson, and Sorensen, 1998.

(18) Kim, H. S., 2001, "Finite Element Analysis of Equal Channel Angular Pressing Using a Round Corner Die," *Mater. Sci. Eng.*, Vol. A315, pp. 122~128.

(19) Lee, S. C. and Kim, K. T., 2002, "Densification Behavior of Aluminum Alloy Powder under Cold Compaction," *Int. J. Mech. Sci.*, Vol. 44, pp. 1295~1308.

(20) Kim, K. T. and Cho, J. H., 2001, "A Densification Model for Mixed Metal Powder under Cold Compaction," *Int. J. Mech. Sci.*, Vol. 43, pp. 2929~2946.

(21) Rice, R. W., 1990, "Toughening in Ceramic Particulate and Whisker Composite," *Ceram. Eng. Sci. Proc.* Vol. 2, No. 7~8, pp. 667~694.

(22) Heoowege, K. H. and Madelung, O., 1984, *Landolt-Bornstein*, Springer-Verlag Berlin.

(23) Lauke, B., Schüller, T. and Beckert, W., 2000, "Calculation of Adhesion Strength at the Interface of a Coated Particle Embedded within Matrix under Multiaxial Load," *Comput. Mater. Sci.*, Vol. 18, pp. 362~380.

(24) Clyne, T. W., 2000, "Comprehensive Composite Materials," *Elsevier Press*, Vol. 3, pp. 95~96.